# Irreversible adsorption of hard spheres at random site (heterogeneous) surfaces

Zbigniew Adamczyk,[a) Paweł Weroński, and Elizeusz Musiał
*Institute of Catalysis and Surface Chemistry, Polish Academy of Sciences, 30-239 Kraków, Niezapominajek 8, Poland*

Irreversible adsorption of hard spheres at random site surfaces was studied theoretically. In contrast to the previous model of Jin *et al.* [J. Phys. Chem. **97**, 4256 (1993)] the dimension of the sites, having the shape of circular disks, was finite and comparable with the size of adsorbing spheres. Adsorption was assumed to occur if the sphere contacted the disk, i.e., when the projection of the sphere center was located somewhere within the disk only. Numerical simulation of the Monte Carlo type enabled one to determine the available surface function, adsorption kinetics, jamming coverage, and the structure of the particle monolayer as a function of the site density (coverage) and the size ratio particle/site, denoted by $\lambda$. It was demonstrated that adsorption kinetics and the jamming coverage increased significantly, at a fixed site density, when the $\lambda$ parameter increased. It was also proven that the results derived from the Jin *et al.* model were valid only if $\lambda > 10$. © *2002 American Institute of Physics.* [DOI: 10.1063/1.1446425]

## I. INTRODUCTION

Adsorption and deposition (irreversible adsorption) of colloids and bioparticles on solid/liquid interfaces is of great significance for many practical and natural processes such as filtration, paper making, thrombosis, protein, bacteria, enzyme immobilization and separation, immunological assays, biofouling of transplants and artificial organs, etc. The efficiency of these processes is usually enhanced by the use of coupling agents preadsorbed at interfaces, which promote attachment of particles. For example, cationic polyelectrolytes are used to increase retention of filler particles (e.g., tiatania) in paper making processes[1] or to promote a selective self-assembly of colloid particles at patterned surfaces.[2,3] In biological applications active ligands are widely applied for a selective binding of a desired solute from protein mixtures, e.g., in the affinity chromatography.[4,5] On the other hand, in the immunological assays[6,7] one often uses colloid particles (polystyrene latex) covered by proteins (antibodies) to detect the presence of antigens in serum. A characteristic feature of these processes is that particle or protein adsorption occurs at surfaces, which are inherently heterogeneous. This raises the important question of what is the relationship between the concentration, size, and distribution of the ligands (which can be treated in the classical adsorption terminology as active centers) and the maximum (jamming) coverage of particles. Also, the kinetic aspects of adsorption at heterogeneous surfaces are interesting from practical viewpoint.

Despite a considerable theoretical significance of these processes, surprisingly few works have been reported in the literature. The exceptions are the papers of Jin *et al.*,[4,8] who studied theoretically irreversible adsorption of disks on non-uniform surfaces covered by point-like adsorption sites. These surfaces were referred to as the random site surfaces (RSS). A correspondence (mapping function) between the adsorption process at nonuniform surfaces and the widely studied random sequential adsorption (RSA) over continuous surfaces[8–12] was found. Both the available surface function governing particle adsorption kinetics and jamming coverage were determined as a function of the dimensionless site density.

The goal of our work is to generalize the results of Jin *et al.*[4,8] to the experimentally more interesting situation when adsorption sites have finite dimensions, comparable with the adsorbing particle size. The range of validity of the approach adopted by Jin *et al.*[4] is determined by performing numerical simulations according to the RSA algorithm. Particle adsorption kinetics, jamming coverage, and structure of the adsorbed layer are derived from these calculations.

## II. THE THEORETICAL MODEL

We consider the following model of irreversible adsorption of spherical particles over heterogeneous surfaces. The ligands (surface heterogeneities) are represented by hard disks of radius $a_s$ and a negligible thickness (see Fig. 1). There are $N_s^0$ disks placed over a homogeneous surface having the geometrical surface area $\Delta S$. Without loss of generality, one can assume $\Delta S = 1$ and normalize accordingly the disk diameter, which was typically $5 \times 10^{-5} - 10^{-9}$ of the simulation area dimension. The surface concentration (2D density) of the disks is then equal to $N_s^0$ and the dimensionless coverage is defined as $\Theta_s = \pi a_s^2 N_s^0$. The configuration of the disks (heterogeneities) can be produced in a number of ways, e.g., by quenching an equilibrium fluid of a given coverage, or by performing RSA simulations, the procedure adopted in our work.

The basic assumption of our model is that the particle can only be adsorbed upon touching the disk, i.e., when the projection of the particle center lies within the disk area (see

a)Electronic mail: ncadamcz@cyf-kr.edu.pl
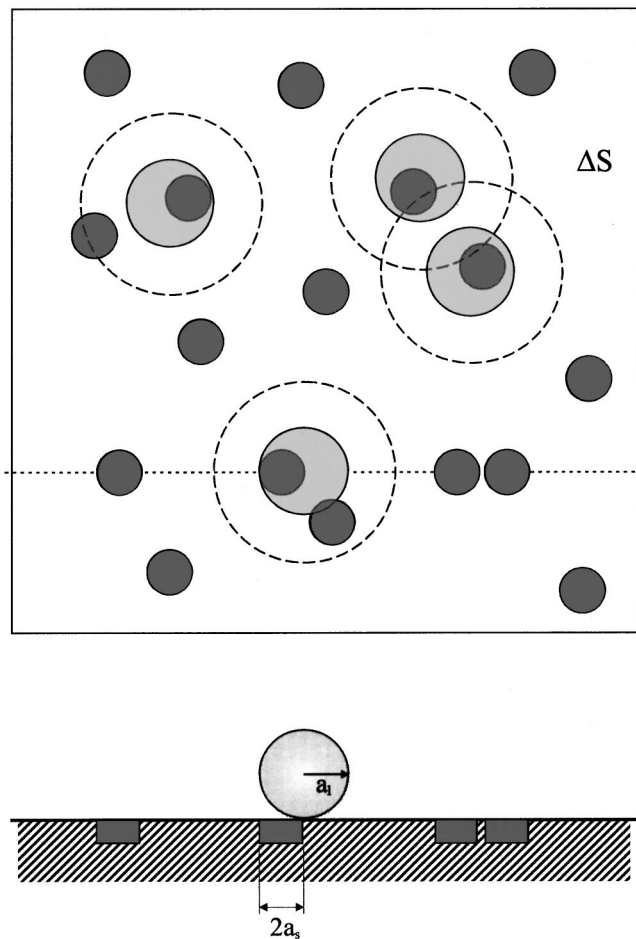
FIG. 1. A schematic representation of particle adsorption over heterogeneous surfaces bearing disk-like adsorption sites.

Fig. 1). Otherwise, at bare interface, the particle will not adsorb. Physically, this corresponds to the situation when the particles are irreversibly bound to the disks due to short-ranged attractive interactions of an electrostatic or chemical nature.

In accordance with this assumption, particle adsorption at the heterogeneous surfaces was modeled as follows:

(i)    An adsorbing (virtual) particle of radius $a_l$ was generated at random within the simulation area with periodic boundary conditions superimposed at its perimeter; if the projection of its center lay outside the area occupied by disks another virtual particle was generated and the number of attempts $N_{att}$ was increased by 1;

(ii)   Otherwise, the overlapping test was performed according to the usual RSA rules, i.e., if any adsorbed particle happened to be within the exclusion area of radius $2a_l$, the simulation loop was repeated (the number of attempts was increased by 1);

(iii)  If there was no overlapping the virtual particle was assumed irreversibly adsorbed at the given position and its coordinates were stored, and the number of adsorbed particles $N_l$ was increased by 1.

As usual in the RSA simulation the dimensionless coverage of particles is expressed as $\Theta_l = \pi a_l^2 N_l$ and the computer adsorption time is defined as[4,8,11,12]

$$t = \pi a_l^2 \frac{N_{att}}{\Delta S} = \pi a_l^2 N_{att}. \tag{1}$$

By plotting $\theta_l$ versus the adsorption time $t$ defined above, one can simulate the kinetics of particle adsorption.

On the other hand, the available surface function (ASF) $\phi$ is defined in our model as

$$\phi = \frac{S_{av}}{\Delta S} = \frac{\Theta_s}{\Delta S} \left( \frac{S_{av}}{\pi a_s^2 N_s^0} \right) = p_0 \bar{\phi}(\Theta_s, \Theta_l, \lambda), \tag{2}$$

where $S_{av}$ is the area where the virtual (wandering) particle can be adsorbed without overlapping (but touching any of the areas covered by disks), $p_0$ is the initial probability of particle adsorption equal to $\Theta_s$ in our case, and $\bar{\phi} = \phi/p_0$ is the normalized ASF.

Our definition of ASF given by Eq. (2) is more general than that introduced by Jin et al.,[4,8] who defined ASF for the discrete random site surface as follows:

$$\phi_J = \frac{N_{av}}{N_s^0}, \tag{3}$$

where $N_{av}$ is the available number of sites at a given coverage of particles.

It should be noted that in the limit of short time, when $\Theta_l \rightarrow 0$, $\bar{\phi} \rightarrow \phi_j$.

Similarly, as in previous works,[10,13] the ASF was calculated by stopping the simulation at a desired coverage $\Theta_l$ and then performing a large number of adsorption trials $N_{att}$ (by keeping $\Theta_l$ constant), $N_{succ}$ of them being potentially successful. Then, $\phi$ is defined as the limit of $N_{succ}/N_{att}$ when the number of attempts tends to infinity (in practice, to a large number equal to $10^5$).

Knowing ASF, one can calculate particle adsorption kinetics by integrating the constitutive dependence[4,10]

$$\phi = \frac{d\Theta_l}{dt}. \tag{4}$$

As discussed in Ref. 14, this classical concept of the ASF may not be general enough to deal with the diffusion-controlled adsorption of particles. More refined approaches, considering a 3D transport of particles, have been proposed.[15–17] Due to insurmountable mathematical problems, their applicability for heterogeneous surface adsorption seems prohibitive. Therefore, in this work, we adopt the standard ASF concept which reflects the most important features of the problem of particle adsorption at heterogeneous surfaces.

The pair correlation function (radial distribution function) $g(r)$ was calculated by generating particle populations according to the above RSA scheme and exploiting the definition

$$g(r) = \frac{\pi a_l^2}{\Theta_l} \left\langle \frac{\Delta N_l}{2\pi r \Delta r} \right\rangle, \tag{5}$$

where $\langle \ \rangle$ means the ensemble average and $N_l$ is the number of particles adsorbed within the ring $2r\Delta r$ drawn around a central particle. Because of the periodic boundary conditions, all particles located closer than $6a_l$ from the perimeter of the simulation area were discarded from the averaging procedure. In order to obtain a satisfactory accuracy of $g(r)$, particle populations reaching $10^5$ were considered.

## III. RESULTS AND DISCUSSION

### A. Limiting analytical expressions

Despite simple rules, the topology and kinetics of particle adsorption at heterogeneous surfaces is rather complex, especially at higher coverage $\Theta_l$. However, two limiting adsorption regimes can be distinguished which can be described by simple analytical formulas. These expressions, having a practical significance, can be exploited for testing the validity of numerical simulations.

The first adsorption regime appears for low coverage of disks (having arbitrary size but smaller than the particles) if one particle blocks upon adsorption only one disk. The criterion for the occurrence of this adsorption regime can be specified by postulating that there is on average less than one disk within the exclusion area $S_e = 4\pi a_l^2$, i.e.,

$$\langle N_e \rangle = S_e N_s^0 = 4\Theta_s \lambda^2 < 1, \tag{6}$$

where $\lambda = a_l/a_s$ is the particle size ratio.
This can be written in concise form as

$$\alpha < \tfrac{1}{4}, \tag{7}$$

where $\alpha = \Theta_s \lambda^2$ can be interpreted as the averaged number of disks found over the interface area having the size of particle cross section $\pi a_l^2$.

Since the adsorbing particle blocks only one disk, the ASF can be expressed as

$$\phi = S_{av} = \pi a_s^2 (N_s^0 - N_l) = \Theta_s \left(1 - \frac{\Theta_l}{\alpha}\right), \tag{8}$$

where $N_l$ is the number of adsorbed particles.

Hence, for $\alpha < \tfrac{1}{4}$ the ASF function is described by the Langmuir model.
Substituting this expression into Eq. (4), one obtains upon integration

$$\Theta_l = \alpha(1 - e^{-\bar{t}/\alpha}), \tag{9}$$

where $\bar{t} = \Theta_s t$ is the normalized adsorption time.

The second adsorption regime, considered by Jin et al.,[4] is realized when the size of the particle becomes much larger than the disk size, i.e., $\lambda = a_l/a_s \gg 1$. Then, the disks can be treated as points (sites) and the available surface area becomes proportional to the number of available sites $N_{av}$ lying outside all exclusion areas; thus

$$\phi = \pi a_s^2 N_{av} = \Theta_s \frac{N_{av}}{N_s^0}. \tag{10}$$

By postulating a uniform distribution of sites, one can demonstrate that[4]

$$N_{av} = (N_s^0 - N_{att})\phi_{RSA}, \tag{11}$$

where $\phi_{RSA}$ is the ASF function for adsorption processes over continuous surfaces governed by the classical RSA model. This is so because particle configuration at a heterogeneous surface bearing $N_s^0$ sites becomes identical for the same coverage $\Theta_l$ with the RSA configuration over continuous surfaces after $N_{att}$ adsorption attempts.[4] The dimensionless adsorption time in the latter case equals $\tau = \pi a_l^2 N_{att}$.

Using Eq. (11), one can express the ASF for the heterogeneous surfaces in the form

$$\bar{\phi} = \phi/\Theta_s = \frac{\alpha - \tau}{\alpha}\phi_{RSA}. \tag{12}$$

This relationship indicates that an unequivocal mapping between adsorption processes at heterogeneous and uniform surface exists if the adsorption time is properly transformed. The time transforming function can be derived from Eq. (12) by noting that for equal coverage

$$\frac{d\tau}{d\bar{t}} = \frac{\alpha - \tau}{\alpha}. \tag{13}$$

By integrating this relationship, one obtains

$$\tau = \alpha(1 - e^{-\bar{t}/\alpha}). \tag{14}$$

One can deduce that for $\bar{t}/\alpha \ll 1$, $\tau = \bar{t}$, which means that adsorption at heterogeneous surfaces becomes practically identical to adsorption on continuous surfaces. On the other hand, for $\bar{t} \to \infty$, $\tau \to \alpha$. This indicates that the jamming state at heterogeneous surfaces corresponds to the adsorption time $\tau = \alpha$ for continuous surfaces, governed by the standard RSA model.

By eliminating $\tau$ from Eq. (12), one obtains

$$\bar{\phi} = \frac{d\Theta_l}{d\bar{t}} = e^{-\bar{t}/\alpha}\phi_{RSA}(\Theta_l). \tag{15}$$

Since this dependence is implicit, one cannot formulate any exact expression for $\phi$ in terms of $\Theta_l$ and $\alpha$.

Equation (15) can be expressed in the integrated form as

$$\int_0^{\Theta_l} \frac{d\Theta'}{\phi_{RSA}(\Theta')} = \alpha(1 - e^{-\bar{t}/\alpha}) = \tau. \tag{16}$$

This relationship can be used for deriving various analytical formulas describing particle adsorption kinetics at heterogeneous surfaces (in the limit of negligible site dimensions). In particular, for the low coverage regime, when[10]

$$\phi_{RSA} = 1 - 4\Theta_l, \tag{17}$$

one can derive from Eq. (16) the expression

$$\Theta_l = \tfrac{1}{4}[1 - e^{-4\alpha(l - e^{-\bar{t}/\alpha})}]. \tag{18}$$

Using this expression to eliminate $\bar{t}$ from Eq. (15) one obtains for $\bar{\phi}$, in the limit of low coverage, the following expression:

$$\bar{\phi}(\Theta_l) = (1 - 4\Theta_l)\left[1 + \frac{1}{4\alpha}\ln(1 - 4\Theta_l)\right]$$

$$\cong (1 - 4\Theta_l)\left(1 - \frac{\Theta_l}{\alpha}\right). \qquad (19)$$

On the other hand, for the long-time regime $\tau \gg 1$, when[8,10]

$$\phi_{RSA} = \frac{1}{2\xi^2}(\Theta_\infty - \Theta_l)^3, \qquad (20)$$

where $\xi = 0.245$ and $\Theta_\infty = 0.547$ is the jamming coverage for the RSA model, one can derive from Eq. (16) the limiting kinetic expression

$$\Theta_l = \Theta_\infty - \frac{\xi}{\sqrt{\alpha(1 - e^{-\bar{t}/\alpha})}}. \qquad (21)$$

The ASF function, for this coverage range, becomes

$$\bar{\phi} = \phi_{RSA}\left[1 - \frac{\xi^2}{\alpha(\Theta_\infty - \Theta_l)^2}\right]. \qquad (22)$$

For arbitrary coverage, the expression for $\phi_{RSA}$ is known in the form of various interpolating functions usually having the form[10,12]

$$\phi_{RSA} = f(\Theta^*)(1 - \Theta^*)^3, \qquad (23)$$

where $\Theta^* = \Theta_l/\Theta_\infty$ and $f(\Theta^*)$ are low-order polynomials.

These formulas can be used in conjunction with Eq. (16) to derive the appropriate kinetic expression. Since this procedure is rather awkward, Jin et al.[4] derived the following function based on interpolation of their numerical results:

$$\Theta_l = \Theta_\infty\left(1 - \frac{1 + 0.314\tau^2 + 0.45\tau^3}{1 + 1.83\tau + 0.66\tau^3 + \tau^{7/2}}\right). \qquad (24)$$

One can use Eq. (24) directly for evaluating particle adsorption kinetics on heterogeneous surfaces for arbitrary range of times by substituting $\tau = \alpha(1 - e^{-\bar{t}/\alpha})$. Consequently, by substituting $\tau = \alpha$, one can calculate from Eq. (24) the jamming coverage $\Theta_l^\infty$ at heterogeneous surfaces. It is interesting to note that for not too large $\alpha$, one can derive from Eq. (24) the simple expression for $\Theta_l^\infty$

$$\Theta_l^\infty = \Theta_\infty\frac{\alpha}{\Theta_\infty + \alpha}. \qquad (25a)$$

On the other hand, for $\alpha \gg 1$, Eq. (24) predicts the asymptotic relationship between the jamming coverage and $\alpha$ in the form

$$\Theta_l^\infty = \Theta_\infty - \frac{\xi}{\sqrt{\alpha}} = \Theta_\infty - \frac{\xi'}{a_l\sqrt{N_s^0}}, \qquad (25b)$$

where $\xi' = \xi/\sqrt{\pi} = 0.138$.
The same result can be obtained from Eq. (21) as well in the limit $\bar{t}/\alpha \gg 1$.

Considering Eq. (25b), one can formulate the expression for $\bar{\phi}$, Eq. (22), in the following form valid for higher coverage:

$$\bar{\phi} = \frac{1}{2\xi^2}(\Theta_l^\infty - \Theta_l)(\Theta_\infty - \Theta_l)(2\Theta_\infty - \Theta_l^\infty - \theta_l)$$

$$= B_1(\alpha)(1 - \Theta^*)(B_2 - \Theta^*)(2B_2 - 1 - \Theta^*), \qquad (26)$$

where $\Theta^* = \Theta_l/\Theta_l^\infty$, $B_1 = [\Theta_l^\infty/2\xi^2]$, $B_2 = \Theta^\infty/\Theta_l^\infty$.

Jin et al.[8] derived a similar interpolating polynomial for $\bar{\phi}$ claimed to be a good approximation for arbitrary range of $\Theta$ and $\alpha$. This function has the form

$$\bar{\phi} = (1 - \Theta^*)(1 - B_1\Theta^* - B_2\Theta^{*2})^2, \qquad (27)$$

where the $B_1$ and $B_2$ are the following functions of $\alpha$:

$$B_1(\alpha) = \alpha\frac{0.713 + 1.4\alpha^{3/2}}{1 + 3.44\alpha + 2.46\alpha^{3/2}},$$

$$\qquad\qquad\qquad\qquad\qquad\qquad\qquad (28)$$

$$B_2(\alpha) = \alpha\frac{0.074 + 0.12\alpha^{3/2}}{1 + 0.544\alpha + 0.27\alpha^{3/2}}.$$

## B. Numerical results

The numerical calculations discussed hereafter, concerning the ASF function, adsorption kinetics, jamming coverage, and pair correlation function, have been carried out for $\lambda = 2$, 5, and 10. This range seems typical for practically occurring situations.

As a preliminary test the simulation algorithm was checked if the ASF in the limit $\Theta_l = 0$ attained the functional dependence predicted theoretically, i.e., $\phi = \Theta_s$. This relationship has a practical significance because the $\phi$ value in the limit of $\Theta_l \to 0$ can be used for calculating the initial flux of solute (particles) to the heterogeneous surfaces. It is interesting to note that in our model, the ASF in the limit $\Theta_l \to 0$ remains smaller than that pertinent to continuous surfaces. This is because the maximum coverage of disks $\Theta_s$ always remains smaller than 0.91 (a hexagonal packing in two-dimension limit). By assuming that the distribution of disks is governed by the RSA model, the maximum value of the initial ASF equals 0.547.

We exploited this initial $\phi$ value to normalize the ASF determined for arbitrary $\Theta_l$, as shown in Figs. 2–4. As one can see in Fig. 2, the dependence of $\bar{\phi}$ on $\Theta_l$ calculated for $\lambda = 2$ can be well described by Eq. (19), provided that $\alpha = \Theta_s\lambda^2 < 0.5$ and $\Theta_l < 0.2$. Thus, this simple analytical expression can be used as a good estimate of the ASF for heterogeneous surfaces in the limit of low $\Theta_l$. It is also interesting to note that the interpolating formula derived by Jin et al.,[4] [Eq. (27)] is not accurate for $\alpha > 0.4$. This suggests that the continuum approach adopted by these authors breaks down for $\lambda = 2$ when the size of the particle is comparable with the size of the adsorption site. Indeed, for larger $\lambda$ the accuracy of the Jin et al.[4] fitting function improves, giving a quantitative agreement with the simulation results for $\lambda = 10$ (cf. Fig. 4). One can, therefore, deduce that for $\lambda > 10$, the reduced ASF function $\phi$ becomes in principle identical with the standard ASF function pertinent to continuous surfaces. It should be remembered, however, that the overall ASF function $\Theta_s\bar{\phi}$ always remains smaller than in
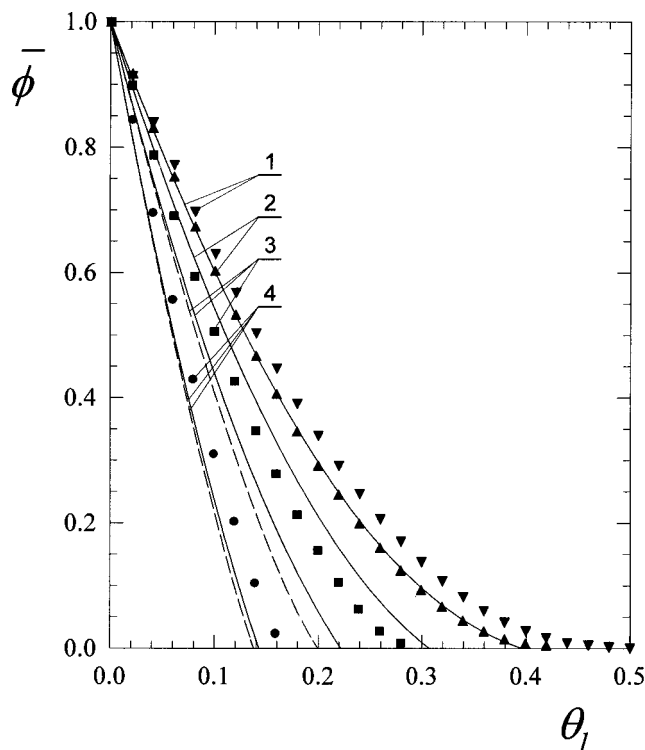
FIG. 2. The dependence of $\bar{\phi}$ on $\Theta_l$ ($\lambda = 2$): (1) ▼, $\Theta_s = 0.5$ ($\alpha = 2$); (2) ▲, $\Theta_s = 0.2$ ($\alpha = 0.8$); (3) ■, $\Theta_s = 0.1$ ($\alpha = 0.4$); (4) ●, $\Theta_s = 0.05$ ($\alpha = 0.2$). The points denote numerical simulations, the solid lines represent the analytical approximation calculated from Eqs. (27) and (28), and the dashed lines shows the results calculated from Eq. (19).
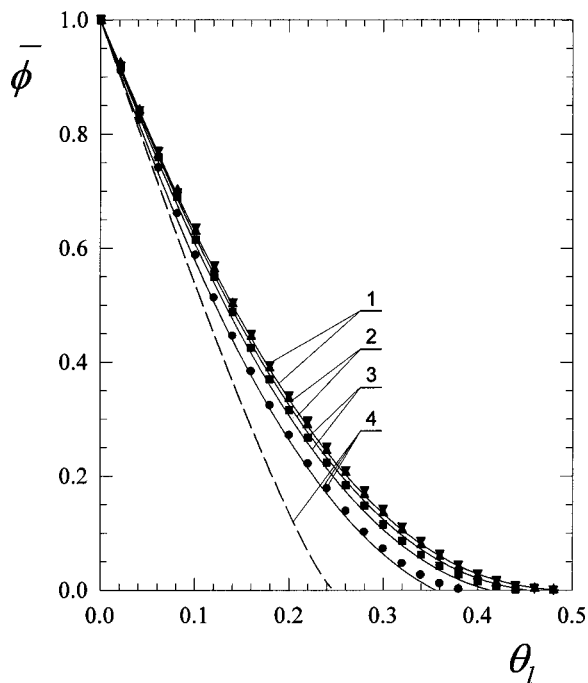


FIG. 3. The dependence of $\bar{\phi}$ on $\Theta_l$ ($\lambda = 5$); (1) ▼, $\Theta_s = 0.5$ ($\alpha = 12.5$); (2) ▲, $\Theta_s = 0.2$ ($\alpha = 5$); (3) ■, $\Theta_s = 0.1$ ($\alpha = 2.5$); (4) ●, $\Theta_s = 0.05$ ($\alpha = 1.25$). The points denote numerical simulations, the solid lines represent the analytical approximation calculated from Eqs. (27) and (28), and the dashed lines shows the results calculated from Eq. (19).
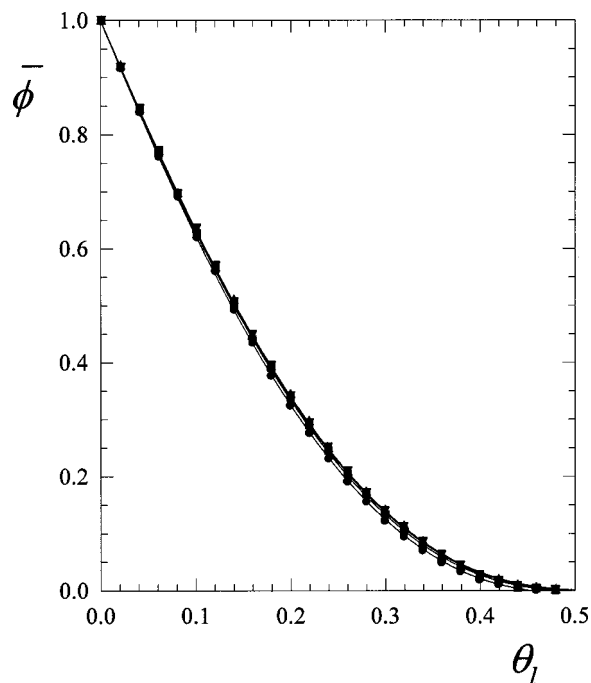


FIG. 4. The dependence of $\bar{\phi}$ on $\Theta_l$ ($\lambda = 10$): (1) ▼, $\Theta_s = 0.5$ ($\alpha = 50$); (2) ▲, $\Theta_s = 0.2$ ($\alpha = 20$); (3) ■, $\Theta_s = 0.1$ ($\alpha = 10$); (4) ●, $\Theta_s = 0.05$ ($\alpha = 5$). The points denote numerical simulations; the solid lines represent the analytical approximation calculated from Eqs. (27) and (28).

the standard RSA model due to the fact that $\Theta_s < 1$. By assuming that the distribution of disks is governed by the RSA model, $\phi = 0.547\phi_{RSA}$.

Apart for calculating the ASF, extensive simulations have been performed for estimating adsorption kinetics of particles. In order to better assess the range of the validity of the random site model of Jin et al.,[4,8] we express these results using the time transformation given by Eq. (14). In this way different numerical runs performed for various $\Theta_s$ can be presented in the form of a universal graph. The numerical data transformed in this way are plotted in Fig. 5 for $\lambda = 2$ and in Figs. 6, 7, for $\lambda = 5$ and 10, respectively. As can be noticed, for $\lambda = 2$ the deviation of our simulations from the theoretical predictions derived for random site surfaces, given by Eq. (24), is considerable. This is especially noticeable for $\tau > 1$. It can be deduced from the data shown in Fig. 5 that the jamming coverage also becomes significantly higher in the case of the discrete site model in comparison with RSA model. This effect can be attributed physically to the fact that due to finite dimensions, a part of the surface of the sites which are located within the exclusion areas remains available for adsorption of additional particles. In the random site model, as a result of negligible dimension of the sites (points), this effect was absent. One can observe in Figs. 5–7 that indeed particle adsorption kinetics is better described by Eq. (24) when $\lambda$ increases (decreasing dimensions of the sites in comparison with particle dimension).

Because the jamming coverage $\Theta_l^{\infty}$ has a fundamental practical significance, we performed extensive simulations aimed at determining this parameter as a function of $\Theta_s$ and $\lambda$. The $\Theta_l^{\infty}$ values were determined from the kinetic runs, i.e., $\Theta_l$ versus $t$ dependencies (with the maximum accessible time
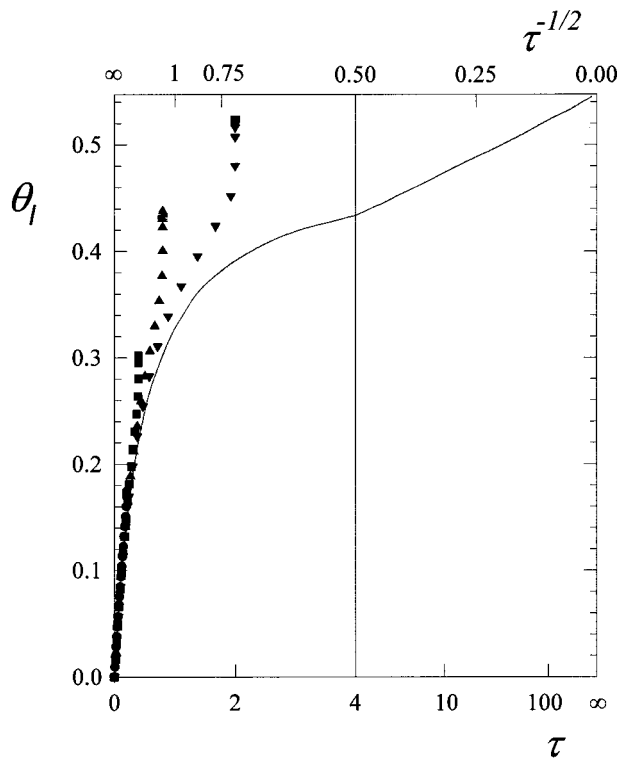
FIG. 5. The dependence of $\Theta_l$ on the transformed adsorption time $\tau = \alpha(1 - e^{-\bar{t}/\alpha})$, $\lambda = 2$; the points denote numerical simulations, performed for $\Theta_s$ equal to 0.02, 0.05, 0.1, 0.2, and 0.5, and the solid line represents the analytical approximation calculated from Eq. (24).
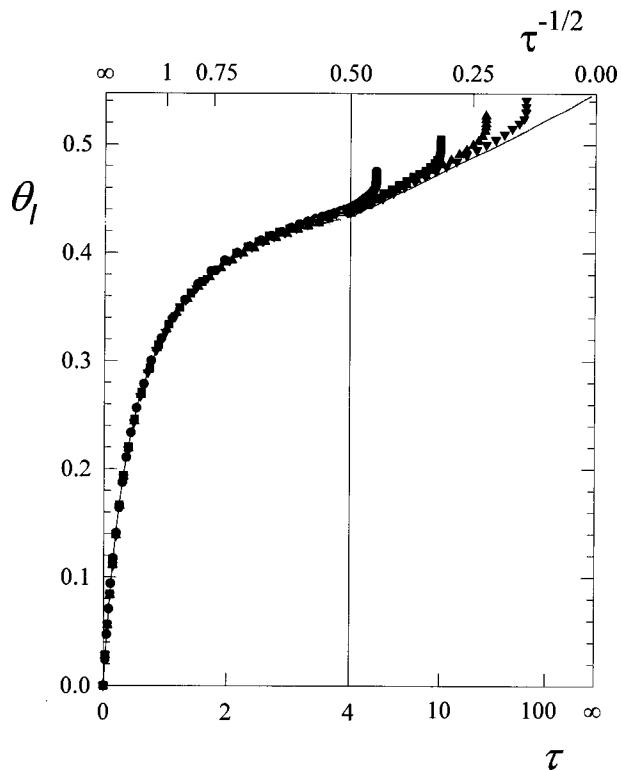


FIG. 7. The dependence of $\Theta_l$ on the transformed adsorption time $\tau = \alpha(1 - e^{-\bar{t}/\alpha})$, $\lambda = 10$; the points denote numerical simulations, performed for $\Theta_s$ equal to 0.02, 0.05, 0.1, 0.2, and 0.5 and the solid line represents the analytical approximation calculated from Eq. (24) (the symbols have the same meaning as in Fig. 5).
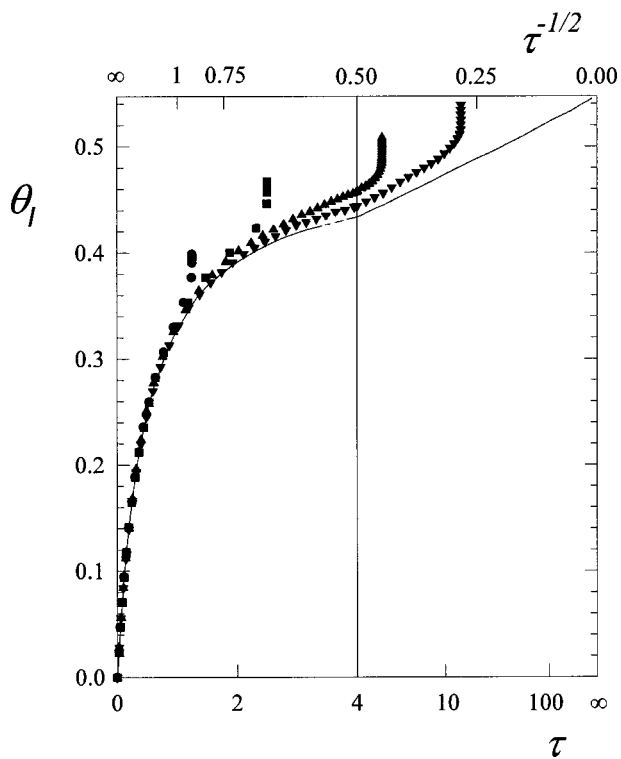


FIG. 6. The dependence of $\Theta_l$ on the transformed adsorption time $\tau = \alpha(1 - e^{-\bar{t}/\alpha})$, $\lambda = 5$; the points denote numerical simulations, performed for $\Theta_s$ equal to 0.02, 0.05, 0.1, 0.2, and 0.5 and the solid line represents the analytical approximation calculated from Eq. (24) (the symbols have the same meaning as in Fig. 5).
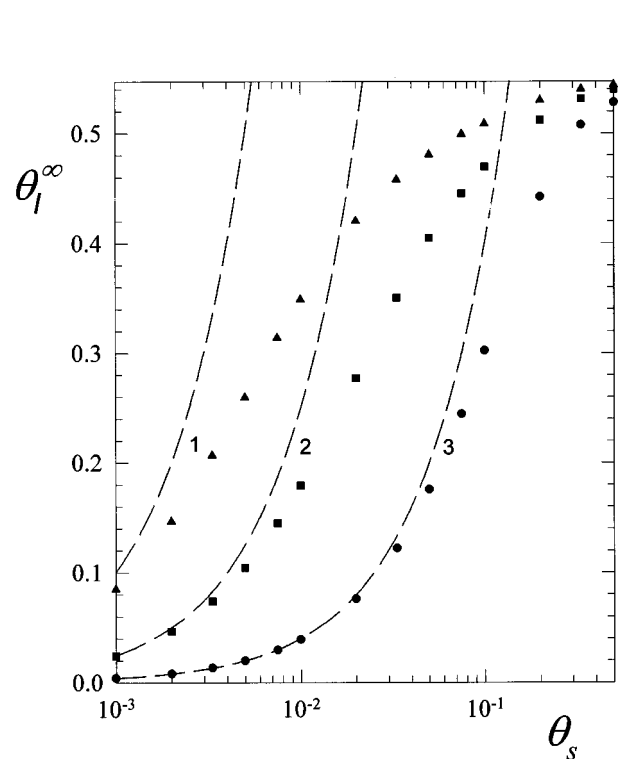


FIG. 8. The dependence of the jamming coverage of particles $\Theta_l^{\infty}$ on the coverage of disks $\Theta_s$; the points denote the results of numerical simulations, performed for (1) ▲, $\lambda = 10$; (2) ■, $\lambda = 5$; (3) ●, $\lambda = 2$. The dashed lines represent the results derived from the Langmuir model, i.e., $\Theta_l = \lambda^2 \Theta_s$.
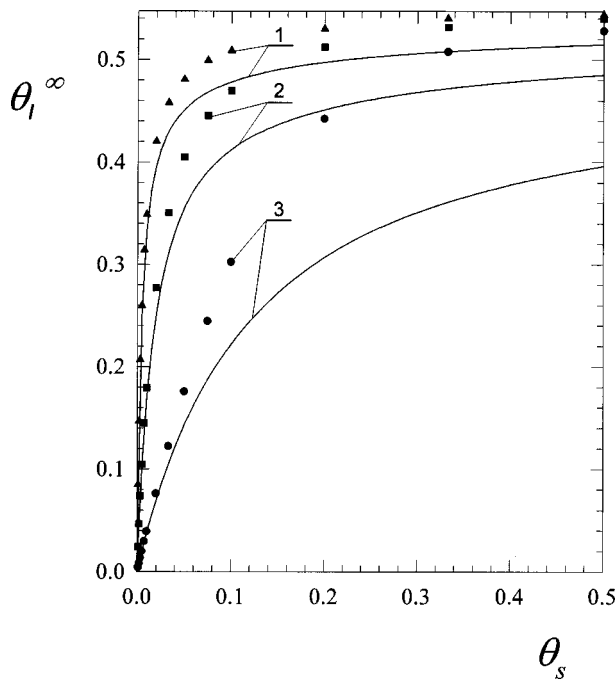
FIG. 9. The dependence of the jamming coverage of particles $\Theta_l^\infty$ on the coverage of disks $\Theta_s$; the points denote the results of numerical simulations, performed for (1) ▲, $\lambda=10$; (2) ■, $\lambda=5$; (3) ●, $\lambda=2$. The solid line represents the analytical results calculated from Eq. (24) by substituting $\tau=\lambda^2\Theta_s$.

about $10^5$) using a linear extrapolation procedure in the $\Theta_l$ versus $t^{-1/2}$ domain. The results plotted as $\Theta_l^\infty$ versus $\Theta_s$ (in logarithmic scale) are collected in Fig. 8. The analytical re-
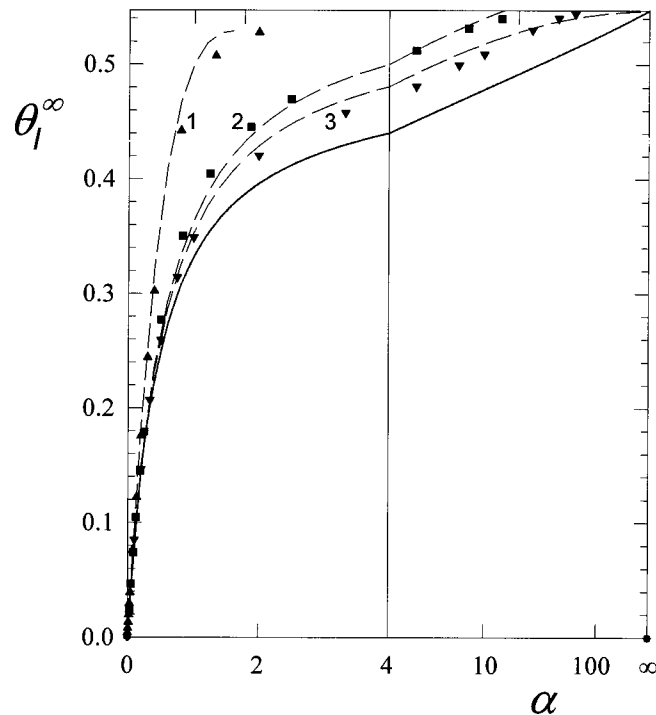


FIG. 10. The universal plot showing the jamming coverage of particles $\Theta_l^\infty$ vs $\alpha=\lambda^2\Theta_s$; the points denote the results of numerical simulations, performed for $\lambda=10$ (inverse triangles), $\lambda=5$ (squares) and $\lambda=2$ (triangles), the solid line represents the analytical results calculated from Eq. (24) by substituting $\tau=\lambda^2\Theta_s$, and the dashed lines show the interpolating results calculated from Eq. (29).
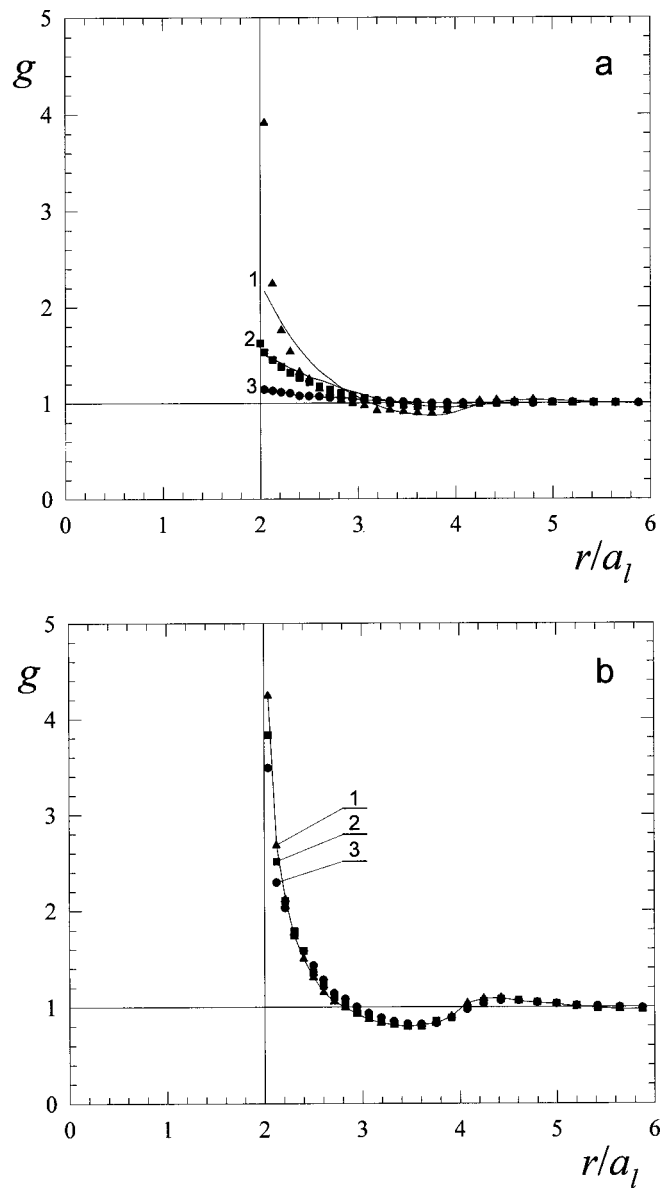


FIG. 11. The pair correlation function of particles $g(r_l)$ derived from numerical simulations for the heterogeneous surfaces: Part a, $\lambda=2$, $\Theta_s=0.2$ (1) ▲, $\Theta_l=0.44$; (2) ■, $\Theta_l=0.3$; (3) ●, $\Theta_l=0.1$. The solid lines denote the results pertinent to uniform surfaces (derived from the standard RSA model). Part b, $\lambda=10$, $\Theta_l=0.5$; (1) ▲, $\Theta_s=0.5$; (2) ■, $\Theta_s=0.3$; (3) ●, $\Theta_s=0.1$. The solid lines denote the pair correlation function pertinent to uniform surfaces (derived from the standard RSA model).

sults predicted from the low coverage dependence, i.e., $\Theta_l=\lambda^2\Theta_s$, are also plotted for comparison. As can be seen, this analytical formula works for $\lambda^2\Theta_s<0.1$ only. In Fig. 9 the same data are plotted in the natural scale $\Theta_l^\infty$ vs $\Theta_s$ and the comparison with the Jin et al.[4] formula [Eq. (24)] is made. As mentioned, the numerical results for finite-sized sites are always larger than the values pertinent to random site surfaces. This effect can be well observed in Fig. 10, where these data are presented using the transformed coordinate system $\Theta_l^\infty$ versus $\alpha=\lambda^2\Theta_s$. As can be seen, even for $\lambda=10$, the numerical data are systematically larger than the limiting analytical results derived from Eq. (24) by substituting $\tau=\alpha$. It was found that a better estimation of the simulations performed for $\lambda=10$ can be attained by using Eq.

(25a). This has a significance in view of the simplicity of this interpolating function, which can be easily applied under practical situations. On the other hand, for smaller $\lambda$, we derived the interpolating function in the form

$$\Theta_l^\infty = \frac{1}{1 + C\alpha^m}, \tag{29}$$

where the constants $C$, $m$ equals 1.75, 1 for $\lambda = 5$ and 1, 3/2 for $\lambda = 2$, respectively.

The structure of the adsorbed particle layers generated in simulation has also been determined for various $\lambda$. As mentioned, in order to attain a satisfactory accuracy of the pair correlation function $g(r)$, particle populations reaching $10^5$ were considered by averaging over many simulation runs. The numerical results plotted in Fig. 11 are compared with the standard RSA results of continuous surfaces. It can be observed that the structure of particle monolayers generated in our simulations is very similar at the same $\theta_l$ to the standard RSA model. Some deviations occur at $\lambda = 2$ and $\Theta > 0.4$ only, when the simulated $g(r)$ is much larger at close separations than its continuous surface counterpart. However, since the range where these deviations appear is much smaller than particle dimension, this effect cannot be easily detected experimentally.

## IV. CONCLUDING REMARKS

It was demonstrated that for particle to site size ratio $\lambda > 10$, adsorption at heterogeneous surfaces (modeled by depositing circular disks of a desired density) can be well reflected by the Jin et al.[4,8] model. Then, a direct mapping between the RSA-RS and the standard RSA model exists. In this case, particle adsorption kinetics and the jamming coverage can be directly calculated from Eq. (24) by introducing the transformed time $\tau = \alpha(1 - e^{-\bar{t}/\alpha})$. On the other hand, the ASF function can be calculated from Eq. (19) for $\Theta_l < 0.2$ and from Eq. (22) for $\alpha \gg 1$. Also, the interpolating function given by Jin et al.,[8] [Eq. (27)] proved a valid approximation.

However, for $\lambda < 5$ the deviations from the RSA-RS model become significant, especially for the jamming coverage, which was found considerably larger (at the same $\alpha$) for the finite disk model. It was found that the jamming coverage can be well approximated for the range of $\lambda$ and adsorption time occurring in practice by the simple interpolating function

$$\Theta_l = \Theta_\infty \lambda^2 / (\Theta_\infty/\Theta_s + \lambda^2).$$

On the other hand, the ASF function can be approximated for arbitrary $\lambda$ and $\Theta < 0.2$ by the limiting formula

$$\phi = \Theta_s(1 - 4\Theta_l)(1 - \Theta_l/\alpha) \cong \Theta_s\left(1 - \frac{4\alpha - 1}{\alpha}\Theta_l\right).$$

Thus, a Langmuir-type form is derived in the limit of low coverage.

It should be remembered that all results discussed in our work are valid for disk distribution governed by the RSA model. It seems that these data also can be used for disk configuration obtained by quenching an equilibrium 2D fluid, in the limit of not too high $\Theta_s$. This is because the pair correlation function in both cases equals $g = 1 + 0(\Theta_s)$ for low coverage.[10] Some differences are expected to appear for higher $\Theta_s$ and $\lambda > 5$. However, a quantitative validation of this hypothesis requires additional numerical simulations.

[1] M. Y. Baluk and T. G. M. van de Ven, Colloids Surf., A **46**, 157 (1990).
[2] S. L. Clark and P. T. Hammond, Adv. Mater. **10**, 1515 (1998).
[3] K. M. Chen, X. Jiang, L. C. Kimerling, and P. T. Hammond, Langmuir **16**, 7825 (2000).
[4] X. Jin, N. H. L. Wang, G. Tarjus, and J. Talbot, J. Phys. Chem. **97**, 4256 (1993).
[5] H. A. Chase, Chem. Eng. Sci. **39**, 1099 (1984).
[6] J. M. Peula, R. Hidalgo-Alvarez, and F. J. D. Nieves, J. Colloid Interface Sci. **201**, 139 (1998).
[7] B. Miksa, M. Wilczyńska, C. Cierniewski, T. Basinska, and S. Slomkowski, J. Biomater. Sci., Polym. Ed. **7**, 503 (1995).
[8] X. Jin, J. Talbot, and N. H. L. Wang, AIChE J. **40**, 1685 (1994).
[9] E. L. Hinrichsen, J. Feder, and T. Jossang, J. Stat. Phys. **44**, 793 (1986).
[10] P. Schaaf and J. Talbot, J. Chem. Phys. **91**, 4401 (1989).
[11] Z. Adamczyk, M. Zembala, B. Siwek, and P. Warszyński, J. Colloid Interface Sci. **140**, 123 (1990).
[12] B. Senger, J. C. Voegel, and P. Schaaf, Colloids Surf., A **165**, 255 (2000).
[13] Z. Adamczyk and P. Weroński, J. Chem. Phys. **108**, 9851 (1998).
[14] B. Senger, P. Schaaf, J. C. Voegel, A. Johner, A. Schmitt, and J. Talbot, J. Chem. Phys. **97**, 3813 (1992).
[15] P. Wojtaszczyk, J. Bonet Avalos, and J. M. Rubi, Europhys. Lett. **40**, 299 (1997).
[16] Z. Adamczyk, B. Senger, J. C. Voegel, and P. Schaaf, J. Chem. Phys. **110**, 3118 (1999).
[17] J. Faraudo and J. Bafaluy, J. Chem. Phys. **112**, 2003 (2000).